Journal of Applied Polymer Science

Effect of chain-extender modification on the structure and properties of thermoplastic poly(ether ester) elastomers

Johnson V. John,[1] Kang Ryul Kim,[1] Seung Tae Baek,[1] Ju Ho Yoon,[2] Hongsuk Suh,[3] Il Kim[1]

[1]BK21 PLUS Center for Advanced Chemical Technology, Department of Polymer Science and Engineering, Pusan National University, Pusan 609-735, Republic of Korea

[2]Enviromental Materials and Components R&D Center, Korea Automotive Technology Institute, Chonan-Si, Chungnam 330-912, Republic of Korea

[3]Department of Chemistry and Chemistry Institute for Functional Materials, Pusan National University, Pusan 609-735, Republic of Korea

Correspondence to: I. Kim (E-mail: ilkim@pusan.ac.kr)

ABSTRACT: The effect of the modulation of a bulky chain extender (CE), 4,8-bis(hydroxymethyl)tricyclo[5.2.1.0(2,6)]decane (TCDO) or hydroquinone bis(hydroxyethyl)ether (HBHEE), on the properties of poly(ether ester) elastomers was investigated. The incorporation of various amounts of TCDO or HBHEE greatly changed the hard-segment (HS) structure and microphase separation behavior; this resulted in a variation of the physical properties, especially for samples with high HS compositions. TCDO and HBHEE were used as minor CEs together with 1,4-butanediol as the major CE for the synthesis of poly(ether ester) elastomers based on the transesterification of dimethyl 2,6-naphthalene dicarboxylate with poly(tetramethylene ether glycol). On the basis of the amount of the minor CE incorporated, samples ranging from an elastomer to thermoplastic. The prepared samples were characterized by various spectroscopic, thermal, and mechanical analyses. The poly(ether ester) elastomers formed honeycomb-structured porous films and microfibers (0.3–1.3 μm in diameter) through the application of a breath figures technique and electrospinning, respectively. © 2015 Wiley Periodicals, Inc. J. Appl. Polym. Sci. **2016**, *133*, 42888.

KEYWORDS: elastomers; esterification; polyesters; step-growth polymerization; synthesis

Received 13 July 2015; accepted 27 August 2015
DOI: 10.1002/app.42888

INTRODUCTION

Segmented thermoplastic poly(ether ester)s (TPEEs) have been widely recognized as an important class of thermoplastic elastomers. TPEE shows an excellent flex fatigue resistance and a broad temperature usage range. It resists tearing, flex-cut growth, creep, and abrasion and shows outstanding toughness while resisting hydrocarbons and many other fluids. It is an attractive material in that its mechanical and thermal properties can be tailored by the modulation of the compositions of soft segments (SSs) and hard segment (HSs).[1–5] Thus, most industrial researches have focused on the modification of the SSs and HSs as a means of improving the mechanical and thermal behaviors of these materials.[6]

Poly(butylene terephthalate) and poly(ethylene terephthalate) were the most frequently used blocks as the HSs in a category of TPEE.[7] Wolfe[8] studied a series of block TPEEs in which the HS was poly(tetramethylene 2,6-naphthalate) and the SS was poly(tetramethylene ether glycol 2,6-naphthalate). Recently, Park *et al.*[9] performed a comparative study of dimethyl 2,6-naphthalene dicarboxylate (NDC) and dimethyl terephthalate using various diol compounds as the chain extenders (CEs) within the HS. The results from the aforementioned studies show that an NDC bearing a diester monomer as the HS improved the mechanical and thermal behavior of TPEEs. Several reports are available on the syntheses of TPEEs with different SSs, such as poly(tetramethylene ether glycol) (PTMEG), poly(ethylene glycol) (PEG), and poly(propylene glycol). Among these, PTMEG was unique for its segmented-block TPEEs as compared with other polyglycols. PTMEG is used as an SS in most commercial TPEEs (e.g., Hytrel by DuPont and Elitel by Elana).[7] In addition, numerous attempts have been carried out with branched TPEEs and polyester with rubber blends to tune the mechanical and thermal behaviors.[10–15] The introduction of a small amount of pentaerythritol or some other polyfunctional monomer was found to instigate TPEE synthesis from PTMEG and PEG into a specific amount of branched chains and influence the physical properties.[14] The multiphase structure and mechanical

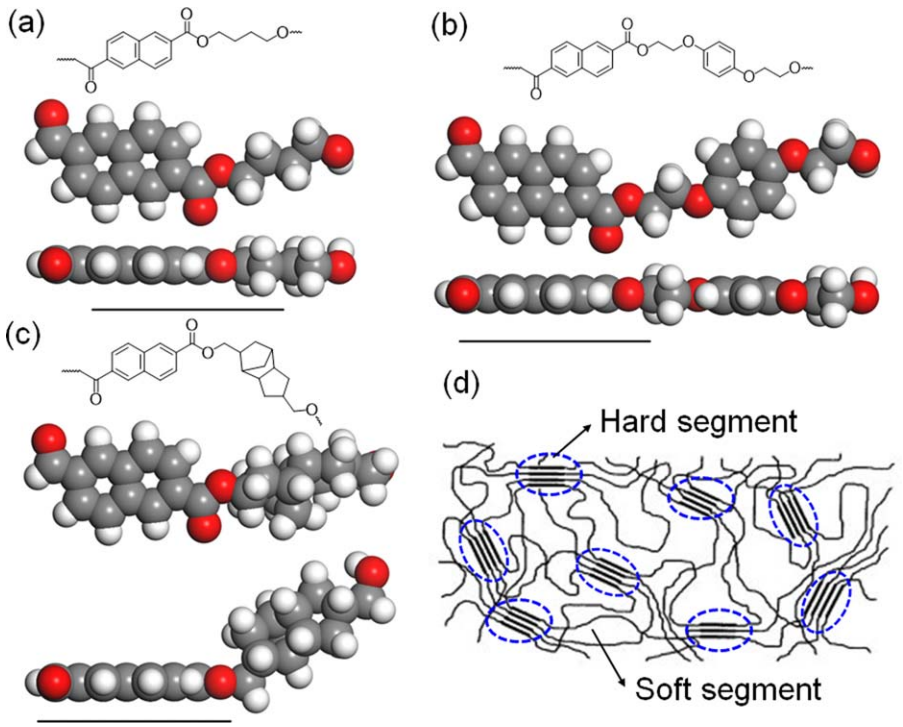

Figure 1. (a–c) Front and side views (space-filling models) of the geometry-optimized structures of HS repeating units formed by different CEs [(a) BD, (b) HBHEE, and (c) TCDO] and (d) microphase separation of HSs. The scale bar represents 1 nm. The energy minimization scans were performed with the Forcite module in Materials Studio 6.0 (Accelrys Software, Inc.).[21] [Color figure can be viewed in the online issue, which is available at wileyonlinelibrary.com.]

properties of TPEEs were also influenced by the effective blending of nitryl rubber into the SS.[16–18]

The aforementioned studies paid little attention to the influence of CE in TPEEs, even though CEs influence the properties of elastomers because of their synchronizing ability in the hard phase. For instance, TPEEs prepared by the reaction of poly(butylene terephthalate) with polyglycol with 2-butyne-1,4-diol as the CE showed much poorer properties than those with 1,4-butanediol (BDO).[19] Interestingly, Nelsen *et al.*[20] demonstrated that the addition of 2-butyne-1,4-diol up to 15 wt % (instead of BDO) during the TPEE synthesis improved its physical and processing properties.

In our study, we chose NDC and PTMEG [molecular weight (MW) = 1000] as the HS and SS, respectively, and BDO as the major CE to synthesize TPEEs. The effect of the modulation of the CE moiety on the properties of TPEE was investigated with 4,8-bis(hydroxymethyl)tricyclo[5.2.1.0(2,6)]decane (TCDO) and hydroquinone bis(hydroxyethyl)ether (HBHEE) as minor CE components together with BDO as the major CE. Because the CE components were incorporated into the HS, the structure of the CE may have influenced microphase separation into domains that were near the block length scales (Figure 1). The resulting HDs, because of various interchain forces, could form crystalline or paracrystalline domains that provided physical crosslinking within the elastomer to reinforce the prevailing rubbery SS matrix. Because the segmented TPEEs consisted of a great number of blocks and the HS may have contained about five repeat units while the soft blocks could have had about 20 repeat units, the microphase segregation, and thus the morphology and physical properties, could be greatly changed. The compositions of TCDO and HBHEE were varied from 10 to 30 mol % with respect to the BDO composition. The TPEEs were characterized by spectroscopy, morphological analysis, thermal and mechanical analyses, and the evaluation of crystallization. As a means of widening the application of TPEE, attempts were made to fabricate honeycomb-structured films and nanofibers with a breath figure lithographic technique[22–24] and typical electrospinning,[25,26] respectively.

EXPERIMENTAL

Materials

Polymerization-grade NDC and PTMEG (MW = 1000) were donated by Kolon Plastics Co. (Gumi, Republic of Korea) and used after drying. TCDO, HBHEE, BDO, titanium tetrabutoxide (97%), and Irganox 1010 were purchased from Sigma-Aldrich and were used as received. Reagent-grade solvents were purchased from Dae Jung Chem. (Republic of Korea) and were purified according to standard procedures before use.

Synthesis of TPEE

The synthesis was carried out in a 1-L high-pressure reactor (Parr Instrument Co.) equipped with a vacuum pump, condenser, and cold trap for collecting the byproducts. TCDO- and HBHEE-bearing PEEs were synthesized with various compositions of [BDO]/[TCDO] or [BDO]/[HBHEE] (see Table I). For example, the initial transesterification of NDC was performed with TCDO/BDO ([NDC]/[CE] = 1.0/1.5) at 60−210°C, and

Table I. Compositions and Physical Properties of TPEEs Prepared through the Modulation of the Minor (TCDO and HBHEE) to Major (BDO) CE Ratio and HS/SS Ratio

HS/SS	Minor CE[a]	Sample code	x_{CE}, minor (%) in the feed[b]	x_{CE}, minor (%) in the polymer[b]	T_{g2} (°C)[c]	T_m (°C)[d]	ΔH_m (J/g)[d]	T_c (°C)[d]	ΔH_c (J/g)[d]	η (dL/g)[e]	$M_v \times 10^{-4}$[e]
50:50	TCDO	5/5PB	0	0	55	202	12.4	140	15.8	1.54	10.1
		5/5PT-10	10	8.3	54	—	—	—	—	1.79	12.7
		5/5PT-20	20	22.1	52	—	—	—	—	1.56	10.5
		5/5PT-30	30	29.2	51	—	—	—	—	1.58	10.6
60:40		6/4PB	0	0	62	210	15.4	143	19.6	1.50	9.8
		6/4PT-10	10	9.1	61	177	4.4	106	5.5	1.37	8.7
		6/4PT-20	20	23	58	—	—	—	—	1.67	11.6
		6/4PT-30	30	41.1	56	—		—	—	1.64	11.1
70:30		7/3PB	0	0	72	225	18.4	175	25.2	1.48	9.3
		7/3PT-10	10	8.1	64	189	8.4	132	10.7	1.46	9.5
		7/3PT-20	20	20.5	57	—	—	—	—	1.61	10.9
		7/3PT-30	30	38.8	56	—	—	—	—	1.52	10.1
50:50	HBHEE	5/5PH-10	10	9.1	53	182	2.6	123	3.5	1.33	8.2
		5/5PH-20	20	23.3	50	—	—	—	—	1.37	8.6
		5/5PH-30	30	39.7	46	—	—	—	—	1.40	8.9
60:40		6/4PH-10	10	10.2	56	185	5.1	120	7.4	1.10	6.3
		6/4PH-20	20	23.6	55	—	—	—	—	1.21	7.2
		6/4PH-30	30	39.8	53	—		—	—	1.26	7.6
70:30		7/3PH-10	10	8	61	192	10.5	131	11.6	1.23	7.4
		7/3PH-20	20	21.7	56	—	—	—	—	1.37	8.6
		7/3PH-30	30	40	53	—	—	—	—	1.42	9.9

[a] Minor CE, TCDO or HBHEE, used together with BD (major CE).
[b] Molar percentage of minor CE (TCDO or HBHEE; e.g., [TCDO]/[TCDO] + [BD]) in the feed and in the polymer (determined by ^{1}H-NMR spectroscopy). [NDC]/[CE] was fixed at 1.0:1.5.
[c] T_g of the amorphous part in the crystalline hard phase. T_{g1}, the T_g of the soft phase, was almost unchanged according with the compositional change.
[d] T_m, crystallization temperature (T_c), ΔH_m, and ΔH_c as measured by DSC.
[e] η and M_v as measured by viscometry.

then, polycondensation with PTMEG was performed at 250–255°C.[27] The TPEEs were purified by precipitation from excess diethyl ether after they were initially dissolved in chloroform. The obtained precipitate was subsequently washed with ethanol and vacuum-dried at 50°C for 24 h.

Fabrication of the Electrospun Fibers

The electrospun fibers were fabricated with NANO NC−ESR 100 (Nano NC, Seoul, Republic of Korea) after the TPEE samples were dissolved in a trifluoroacetic acid/dichloromethane (8:2 v/v) mixture at a concentration of TPEE of 30% w/v according to reported procedures.[27] The fiber morphology was investigated with scanning electron microscopy (SEM; Hitachi S-3000H, Japan). Before the analysis, the samples were fixed to copper stubs with carbon adhesive tape and sputter-coated with 10-nm gold particles.

Fabrication of the Honeycomb Films

To fabricate the honeycomb pattern, TPEE was dissolved in $CHCl_3$ (0.1 g/dL), and the solution was dropped onto a clean cover glass (18 × 18 mm^2) in an acrylic humidity chamber.[27] An optical microscope (Eclipse 80i, Nikon Co., Japan) with 100 and 1000× magnifications was equipped with transmittance and reflective modes and used to observe the surface morphologies of the porous honeycomb films. Further analysis of the surface morphologies of the porous honeycomb films was made with SEM.

Characterization

The intrinsic viscosity (η) of TPEE was measured at 30°C with a capillary Ubbelohde-type viscometer. The polymer concentration was maintained at 0.5 g/dL in a phenol/1,1,2,2-tetrachloroethane (60:40 v/v) mixture. The viscosity-average molecular weight (M_v) was estimated with the Mark–Houwink equation ($\eta = KM_v^a$, where $K = 5.36 \times 10^{-4}$ and $a = 0.69$).[28] The values of the Mark–Houwink parameters, a and K, depend on the particular polymer-solvent system. ^{1}H-NMR (400 MHz) and ^{13}C-NMR (100 MHz) spectra were recorded on a Varian Inova 400 NMR spectrometer. Fourier transform infrared spectra were recorded on a Shimadzu IRprestige-21 spectrophotometer at room temperature. The spectra were recorded with KBr pellets

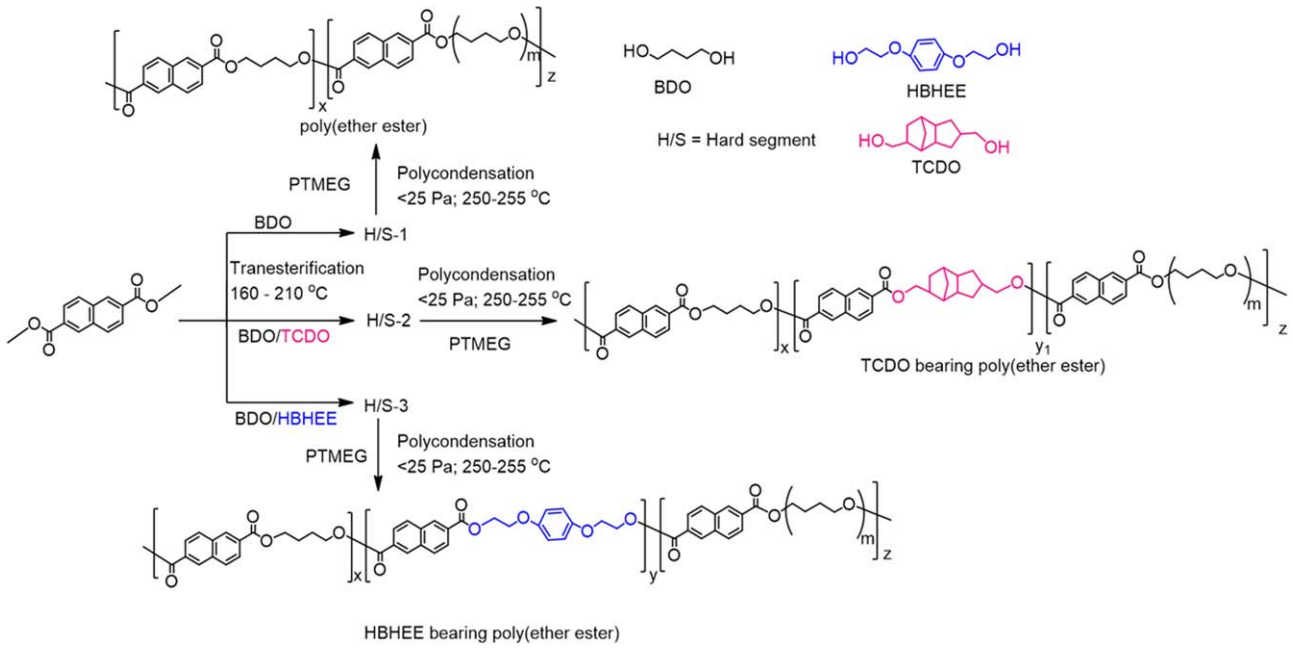

Scheme 1. Synthesis of poly(ether ester)s with various CE formulations: BDO, BDO/TCDO, and BDO/HBHEE. [Color figure can be viewed in the online issue, which is available at wileyonlinelibrary.com.]

with a scanning range of 4000−500 cm^{-1}. Raman spectra of the TPEE films (thickness = 0.2 mm) were recorded in a Senterra dispersive Raman microscope (System 3000) containing an Olympus metallurgical microscope and a charge-coupled device detector with 785-nm exciting radiation (He–Ne laser, Spectra Physics, model 127). The laser beam was focused on the sample in an approximately 1-μm spot by a 10 × 50 lens. The laser power was always kept below 0.7 mW at the sample to prevent its degradation. All atomic force microscopy images were recorded with a Bruker Neos Senterra atomic force microscopy system in tapping mode. A silicon cantilever with a bending spring constant of 20–60 N/m and a resonance frequency of about 250–350 kHz was used for imaging at scan rate of 0.5 Hz. The TPEE films (thickness ≈ 50 nm) were annealed at different temperatures for 2 h, and then, they were quenched with liquid nitrogen. Gwyddion image processing software was used for the analysis of the observed surface structures. The tensile properties of the samples were measured with a KSU05 (Kyungsung Testing Machine Co., Republic of Korea) at a constant crosshead speed of 100 mm/min. The analysis was performed at room temperature on uniformly shaped specimens. At least three specimens were tested for each given value. The elongation percentage and ultimate strength were measured from the stress–strain curves. Differential scanning calorimetry (DSC) measurements were carried out on a Q100 instrument (TA Instruments) in temperatures of −30 to 280°C and at a heating–cooling–heating rate of 10°C/min. The glass-transition temperature (T_g) and melting temperature (T_m) were determined from the temperature–heat flow graph. Wide-angle X-ray scattering (WAXS) measurements of the samples were carried with a Bruker D8 Advance diffractometer equipped with computerized data collection and analytical tools. The X-ray source, Cu Kα radiation with a wavelength of 1.54 Å, was generated with an applied voltage of 40 kV and a filament current of 40 mA. Cu Kα radiation was monochromatized with a graphite monochromatizer and Ni filter. The XRD patterns were recorded in the 2θ range of 10–60° with a step size of 0.02°. The storage modulus (E'), loss modulus (E''), and loss tangent (tan δ) values were measured on a Q800 dynamic mechanical thermal analyzer (TA Instruments) working in tension mode at a frequency of 1 Hz. The samples were first cooled to −100°C and then subsequently heated at a rate of 2°C/min. T_g was taken as the temperature at the maximum relaxation peak of the E'' and tan δ curves.

RESULTS AND DISCUSSION

To analyze the efficacy of CE modification in the modulation of physical properties of TPEE, TCDO bearing a bulky tricyclo[5.1.0–2.6]decane ring and HBHEE bearing phenyl ring were chosen as minor CEs. These CE components were incorporated into NDC units together with BDO by initial transesterification and subsequent polycondensation in the presence of titanium tetrabutoxide (Scheme 1). Three series of TPEEs were synthesized through the control of the HS/SS composition ratio at 50:50, 60:40, and 70:30. In each series, the [TCDO]/[BDO] or [HBHEE]/[BDO] ratio was formulated as 10:90, 20:80, and 30:70. Step-growth polycondensations were performed in the molten state with BD (and TCDO or HBHEE), PTMEG, and NDC in two stages: (1) transesterification of NDC with the hydroxyl groups of low-MW diols and (2) melt polycondensation at high temperatures (250–255°C) under dynamic vacuum (Scheme 1).

Usually, the first stage of transesterification is carried out in excess CE to a conversion level of over 90%. The amount of methanol generated during the reaction was used to control the extent of the reaction. In the stage of polycondensation, after the introduction of a prescribed amount of PTMEG into the

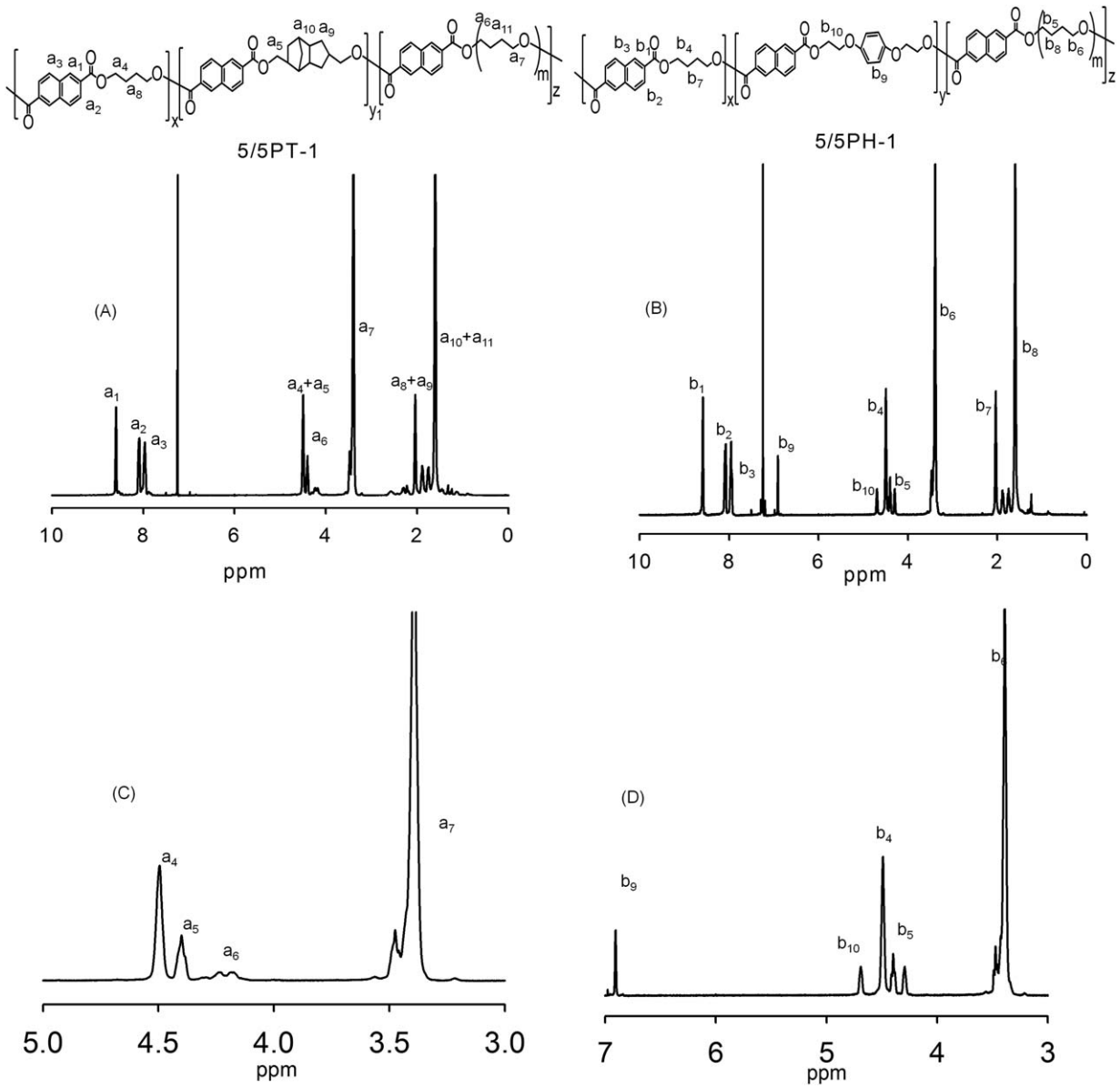

Figure 2. [1]H-NMR spectra of the (a) 5/5PT-10 and (b) 5/5PH-10 samples.

reactor, together with a catalyst and an antioxidant, the reaction mixture was heated slowly to 250–255°C under a reduced pressure. Evidently, the transesterification of NDC with CE ceased under these conditions, and further oligomerization occurred by ester exchange. The removal of unreacted BDO from the reaction medium under the reduced pressure brought the reaction to completion. The polymerization results are summarized in Table I. TPEE is abbreviated as PT for the sample bearing TCDO and as PH for the sample bearing HBHEE. For example, the 5/5PT-10 sample was prepared by the control of the relative amount of TCDO to 10% and by the modulation of the HS/SS ratio to 50:50. The η values of the PT samples were in the range 1.37–1.79 dL/g; this corresponded to 87,000–127,000 M_v values. The η values were in the range 1.10–1.42 dL/g for the PH samples; this corresponded to 63,000–101,000 M_v values. These results clearly show that high-MW TPEEs were achieved with the polymerization conditions used in this study.

In a comparison of TPEEs prepared with only BDO, MW (as M_v) decreased as HS increased for both the PT and PH series of samples. In general, the PT samples showed higher MWs than the PH samples prepared with similar relative formulations. Even though the MW values were also dependent on the relative amount of minor CEs, there were no mentionable trends in each series of samples.

The relative CE compositions in the TPEEs, the TCDO/BDO and HBHEE/BDO ratios, were estimated by a comparison of the integral intensities of the [1]H-NMR spectra [Figure 3(C,D)],[29] that is, by the integration of the a_4, a_5, and a_7 peaks in the PT samples and the b_9, b_4, and b_6 peaks in the PH samples. The results are also summarized in Table I. As [TCDO]/

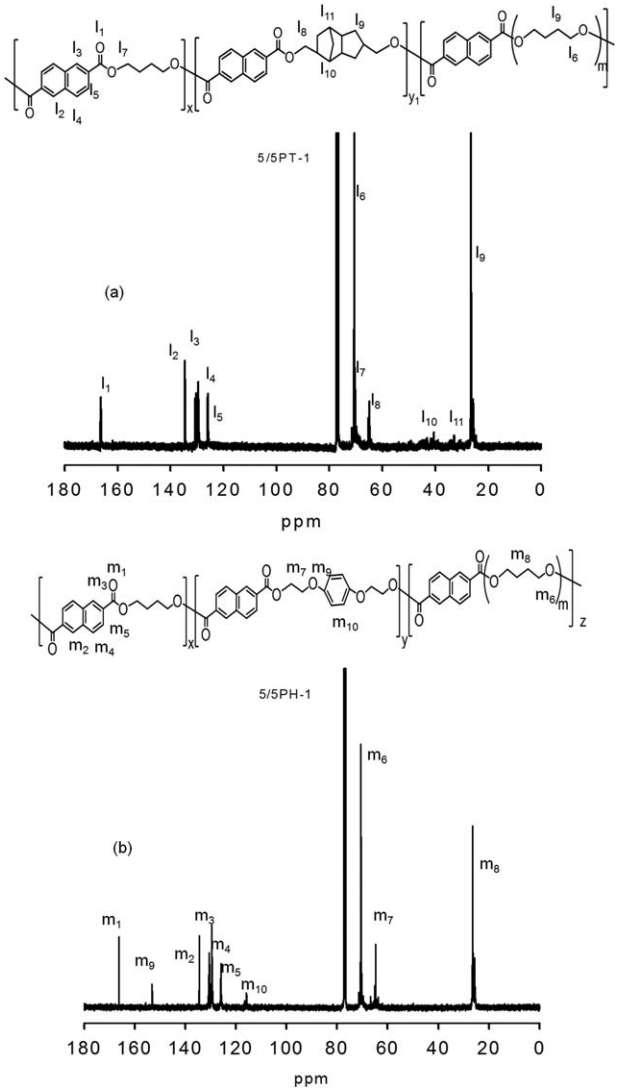

Figure 3. ^{13}C-NMR spectra of the (a) 5/5PT-10 and (b) 5/5PH-10 samples.

[BDO] or [HBHEE]/[BDO] in the feed increased, the relative amount of TCDO or HBHEE incorporated in the polymer backbones increased accordingly; this demonstrated that both TCDO and HBHEE showed no problem in reactivity because they bore primary hydroxyl groups like BDO.

Structural Analysis by Spectroscopy

The TPEE structures were confirmed by ^{1}H-NMR and ^{13}C-NMR spectroscopies. The ^{1}H-NMR spectrum of the 5/5PT-10 sample [Figure 3(A)] showed chemical shifts (8.62, 8.09, and 7.97 ppm) assigned to the aromatic protons of naphthalate. The chemical shifts at 4.39 and 1.91 ppm were assigned to the methylene protons of BDO (CH_2—CH_2—CH_2—CH_2 and CH_2—CH_2—CH_2—CH_2, respectively). The signals at 3.45 and 1.63 ppm represented the methylene protons of PTMEG (CH_2—CH_2—CH_2—CH_2—O and CH_2—CH_2—CH_2— CH_2—O, respectively) repeating blocks. The signal at 4.56 ppm corresponded to the methylene proton of TCDO (CH—CH_2—O) outside the cycle, and all of the remaining protons of TCDO produced shifts at less than 2.3 ppm. Figure 3(B) depicts the ^{1}H-NMR spectrum of the 5/5PH-10 sample, where many of the shifts were similar to those of the TCDO-incorporated PEEs, including the aromatic protons of naphthalate, BDO, and PTMEG. However, the chemical shift at 6.95 ppm indicated the phenyl proton of the HBHEE moiety, and the one at 4.70 ppm corresponded to the methylene protons of HBHEE (O—CH_2—CH_2—O).

The ^{13}C-NMR spectrum of the 5/5PT-10 sample [Figure 4(a)] showed the following signals: 166.66 ppm for the *C*(O)O carbon and 134.99, 131.49, 129.71, and 125.88 ppm for the carbons of the naphthalate units. Similarly, the signal at 70.41 ppm corresponded to the carbon of PTMEG (CH_2—CH_2— CH_2—CH_2—O). The chemical shift at 64.84 ppm represented the carbons of the BDO (CH_2—CH_2—CH_2—CH_2) unit, and that at 26.67 ppm showed the carbons of PTMEG (CH_2—CH_2—CH_2—CH_2—O) and BDO (CH_2—CH_2— CH_2—CH_2). The methylene carbon (CH—CH_2—O) of the TCDO segment appeared 65.32 ppm. The remaining carbons of TCDO exhibited shifts ranging between 27 and 45 ppm.

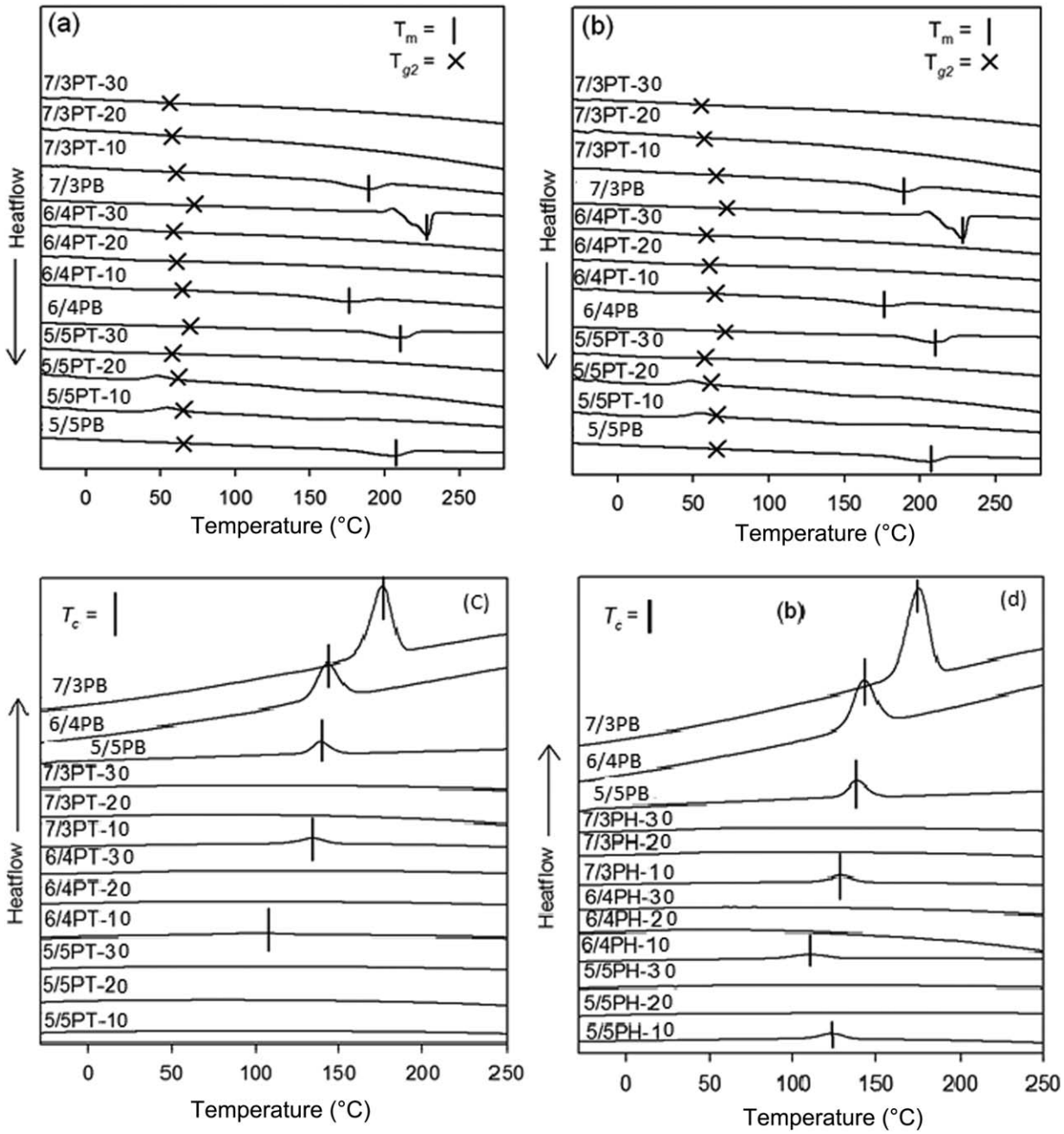

Figure 4. (a) DSC exotherms and (b) DSC endotherms of TPEEs with various CE compositions and SS/HS ratios at a heating rate of 10°C/min.

Figure 4(b) shows the ^{13}C-NMR spectrum of the 5/5PH-10 sample. The aromatic carbons of the naphthalate units and the carbons attributed to BDO and PTMEG exhibited similar shifts as the 5/5PH-10 sample. However, the chemical shift at 153.69 ppm represented the ortho and para carbons of the phenyl group in HBHEE, whereas the chemical shift at 116.01 represented the other carbons of the phenyl group, and those at 66.32 and 63.45 ppm represented the methylene carbons of HBHEE (O—CH_2—CH_2—O).

Thermal Properties and Crystallinity

The DSC exotherms and endotherms of the two series (PT and PH) of samples are shown in Figure 5. TPEEs prepared with only BDO were also measured for comparison. In general, the phase structure and morphology of the elastomers were dependent on the thermodynamic immiscibility of rigid HSs and flexible SSs. Typical elastomers consist of an SS-rich region (T_{g1}, glass transition temperature of SS), a region of SSs blended with HSs (T_{g2}, glass transition temperature of amorphous part in crystalline HS), and an HS-rich region (T_m). The T_m and T_g values measured by thermal analysis at temperatures between −30 and 280°C are also summarized in Table I. In the PB samples, the T_m value increased as the composition of HSs increased; that is, the values were 202, 210, and 225°C for 5/5PB, 6/4PB, and 7/3PB, respectively. Even though the T_{g1} value was almost unchanged (appearing between −50 and −40°C

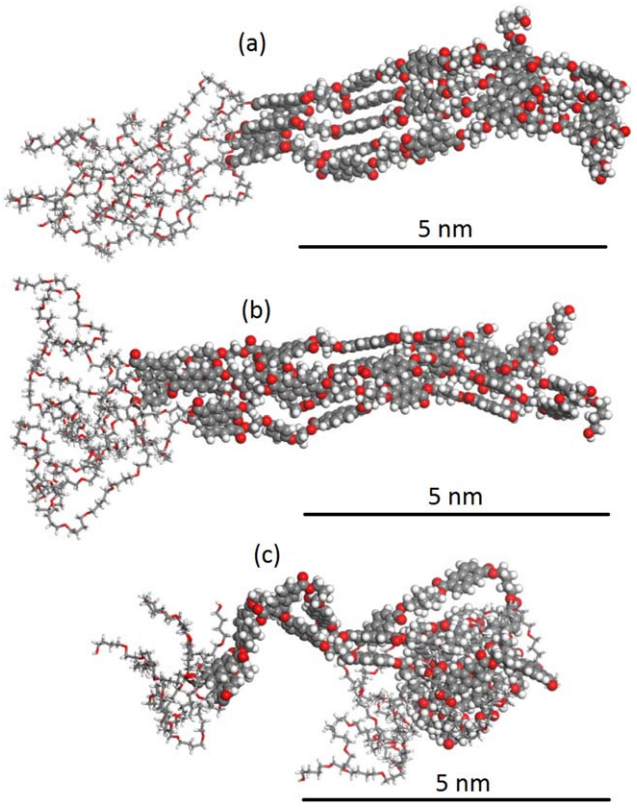

Figure 5. Energy-minimized structures of five packed block units. One block unit consisted of a PTMEG SS and an HS moiety: (a) five NDC–BDO adducts, (b) four NDC–BDO units with a randomly distributed NDC–HBHEE adduct, and (c) four NDC–BDO units with a randomly distributed NDC–TCDO adduct. [Color figure can be viewed in the online issue, which is available at wileyonlinelibrary.com.]

according to the compositional change because all of the samples used PTMEG as an SS component), the T_{g2} value increased as the composition of HSs increases; that is, the values were 55, 62, and 72°C for 5/5PB, 6/4PB, and 7/3PB, respectively.

In the PT series of samples, the T_{g2} value decreased monotonously as the relative composition of TCDO increased, regardless of the HS/SS ratio; this was most probably due to the increase of randomness of the backbone caused by the bulky TCDO. The fact that only 7/3PT-10 and 6/4PT-10 had discernible T_m values at 189 and 177°C, respectively, showed the failure of tight interchain packing of HSs. Similar phenomena were observed for the3 PH series of samples, even though these contained planar HBHEE as a minor CE. Samples with low amounts of HBHEE, such as 5/5PH-10, 6/4PH-10, and 7/3PH-10, showed clear melting transitions. The T_{g2} value decreased as the relative composition of HBHEE increased as well. It was evident that the CE composition affected T_{g2} because of region consisting of an SS blended with an HS. Interestingly, the 5/5PH-10 sample showed a T_m value at 182°C, whereas the 5/5PH-10 sample showed no melting transition. Even though parts of the PT and PH series of samples showed melting transitions, the degree of crystallinity was expected dramatically decrease as the content of minor CEs increased; this could be seen clearly in a comparison of the enthalpy of melting (ΔH_m) and enthalpy of crystallization (ΔH_c) values of the polymers.[27]

Segmented TPEEs are multiphase systems with a blurred separation surface. As a result, the properties were deeply influenced by their molecular structure and specific physical microstructure, which resulted from the microphase separation of HS and SS blocks; this was a consequence of the differences in the constitution of each block. To obtain some insights into the effect of the molecular structure of the HS block on the microphase separation, a molecular dynamics simulation was performed. After the packing of five block units consisting of an HS and a PTMEG molecule (MW = 1000) roughly corresponding to an HS/SS of 5:5, where the HS consisted of one unit of a randomly distributed TCDO- or HBHEE-incorporated HS within four units of a BDO-incorporated HS, energy minimization was conducted with Materials Studio version 6.0, with the anneal and geometry optimization tasks in the Forcite Plus module (Accelrys Software, Inc.).[21] An initially energy-minimized packed block unit was subjected to 400 annealing cycles with initial and midcycle temperatures of 50 and 1400 K, 20 heating ramps per cycle, 1000 dynamics steps per ramp, and one dynamics step per femtosecond. A constant volume/constant energy ensemble was used; the geometry was optimized after each cycle. All of the geometry optimizations used a Dreiding force field and a Gasteiger charge with atom-based summation and cubic spline truncation for both the electrostatic and van der Waals parameters. Figure 6 shows the layered packing state after annealing dynamics simulations. The block unit consisting of a PTMEG and five BDO–NDC condensates showed a regular arrangement between SSs and HSs because of various interchain interactions. On the other hand, the incorporation of an HBHEE, especially a TCDO, into the HS units greatly increased the randomness of the block unit. The increase of randomness and, thus, the increase in entropy must have been an unfavorable factor for the microphase separation through the decrease in the change in the Gibbs free energy of mixing. The failure in microphase separation made the whole polymer matrix thermoplastic rather than elastomeric.

The loss of crystallinity through the addition of TCDO and HBHEE was easily identified by WAXS measurements (Figure 7). The samples prepared with only BDO, 5/5PB, 6/4PB, and 7/3PB showed characteristic peaks that indicated crystalline phases. For example, 7/3PB showed characteristic peaks at scattering angles of 11.56, 12.79, 14.87, 20.64, 23.22, and 29.53° (d-spacing = 0.766, 0.70, 0.59, 0.53, 0.42, and 0.37, respectively), corresponding to the lattice reflection planes of (010), (01$\bar{2}$), (1$\bar{0}$1), (100), (11$\bar{3}$), and (11$\bar{1}$).[7,29] However, the characteristic peaks were broadened for the samples prepared by the incorporation of minor CEs. The peak broadening was more evident for the PT series of samples. These results were in line with those obtained from thermal analysis and molecular dynamics simulations.

Dynamic Mechanical Thermal Analysis (DMTA)

DMTA was used to investigate the relaxation mechanism and consequently elucidate the microphase separation of the block polymer systems. Figure 8 shows the evolution of the E' and tan δ

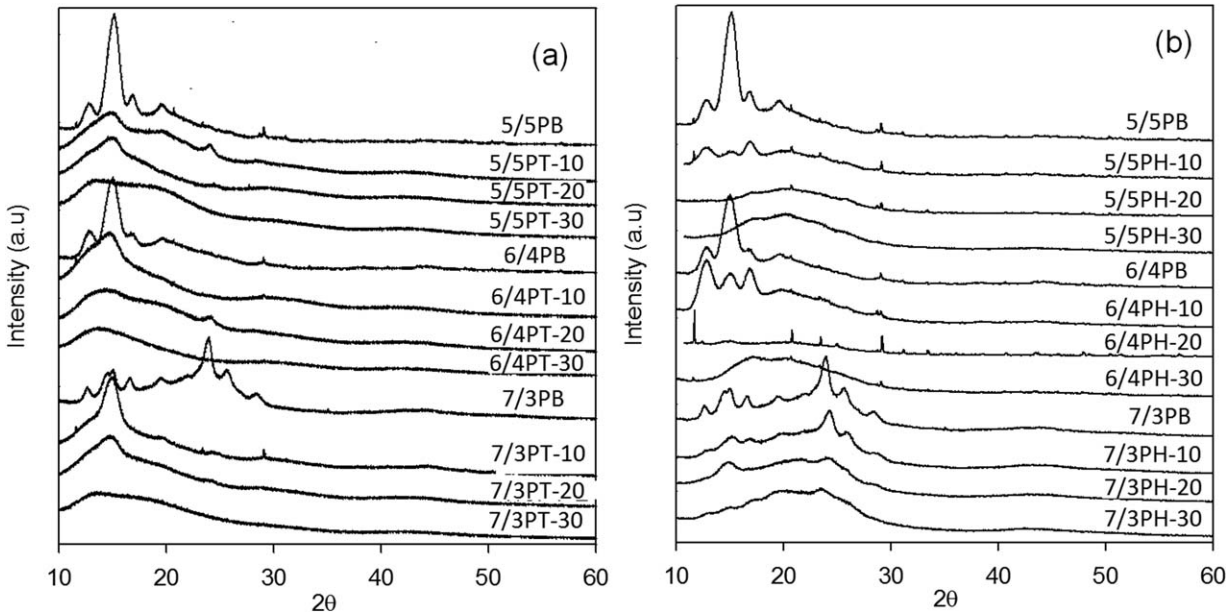

Figure 6. WAXD curves of TPEEs with various CE compositions and SS/HS ratios.

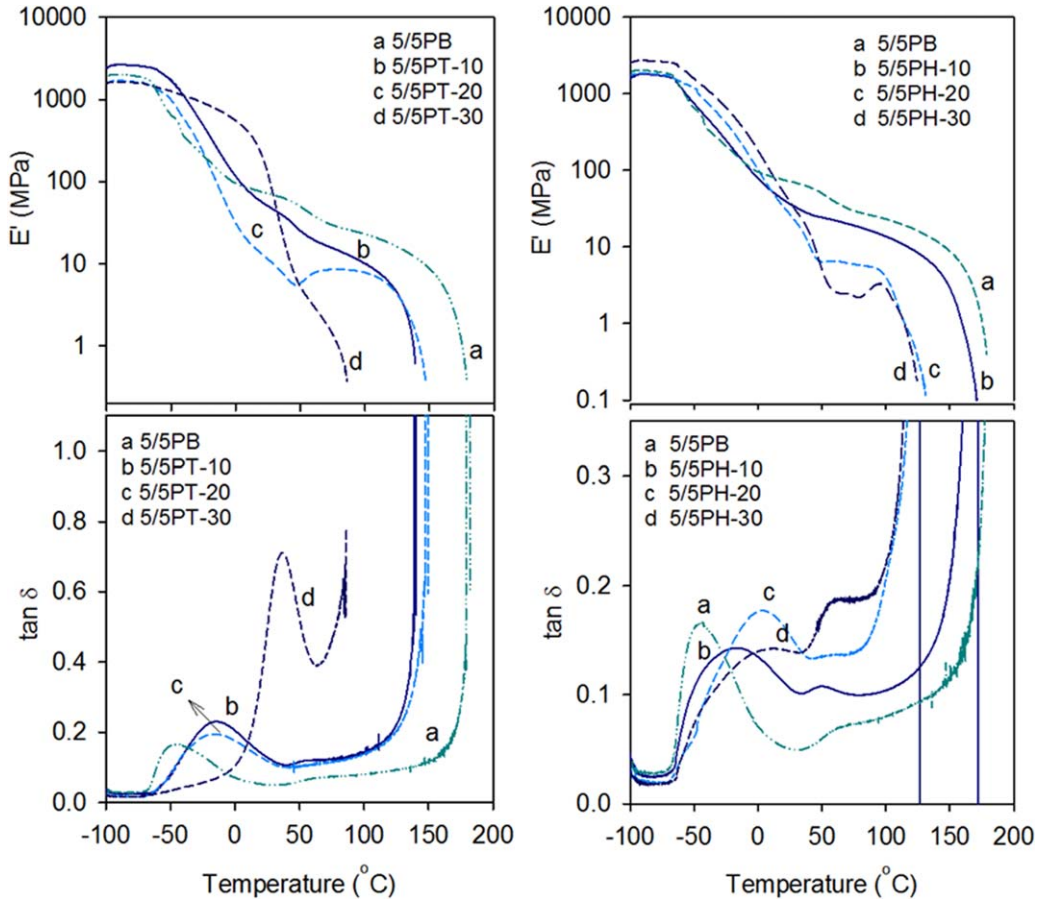

Figure 7. E' and tan δ values obtained from the DMTA scans of slowly cooled PT and PH series of samples with a 50:50 SS/HS ratio. [Color figure can be viewed in the online issue, which is available at wileyonlinelibrary.com.]

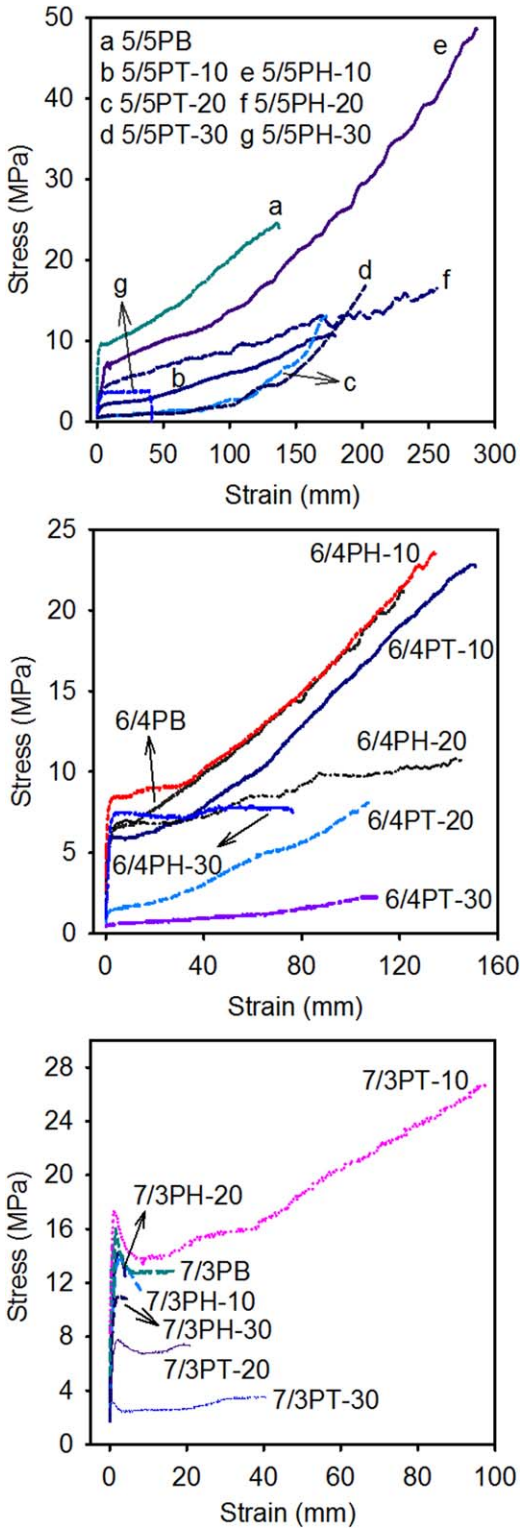

Figure 8. Stress–strain curves of TPEEs with various SS/HS ratios [50 : 50 (top), 40 : 60 (middle), and 30 : 70 (bottom)] in the presence of different amounts of TCDOs and HBHEEs as the minor CEs. [Color figure can be viewed in the online issue, which is available at wileyonlinelibrary.com.]

signals with temperature for an HS/SS ratio of 50:50. A drop in E' and a peak in the tan δ curve represented the relaxations. In brief, beginning at about −100°C, the sample underwent an initial softening; this arose from the glass-transition behavior of the PTMEG segment. This glass transition was distinctive for all of the series of materials because the same type and amount of PTMEG were used to prepare the samples and it had to be the glass transition of the PTMEG-rich phase. This relaxation could overlap with a secondary relaxation caused by local motions of the ester groups. After this transition, a rubbery plateau behavior in the modulus was apparent from about 0 to 150°C. This plateau region corresponded to the service temperature window for many of the applications of these materials because there was a relatively low dependence of stiffness on the temperature. The transition between −20 and 50°C for the 5/5PB, 5/5PH-10, and 5/5PT-10 samples most probably corresponded to the glass transition of the ester-rich phase. After the rubbery plateau region, a decline in E' occurred because of the melting of the HS. In a comparison of 5/5PB with the 5/5PH-10 or 5/5PT-10 sample, the 5/5PH-10 sample showed distinct transitions like those of 5/5PB; however, the boundary between transitions became sharply narrow for the 5/5PT-10 sample. As the amount of minor CE increased, the resulting samples represented only negligible rubbery plateaus. The attribution of two well-separated glass transitions to the respective amorphous polyester- and polyether-rich regions resulted from a well-defined microphase separation inside the amorphous regions. In this sense, the samples prepared with larger amounts of minor CE, 5/5PT-20, 5/5PT-30, 5/5PH-20, and 5/5PH-30, showed only poor microphase separation.

With the composition of TPEEs in this study, there coexisted three microphase-separated phases: (1) a PTMEG amorphous phase with a small amount of isolated polyester segments dissolved therein, (2) a polyester amorphous phase in which the concentration of the mixed PTMEG segments depended on the PTMEG content, and (3) a polyester crystalline phase that melted above 200°C. The addition of TCDO and HBHEE as the minor CEs increased the polyester amorphous phase because of their steric and conformational effects; this resulted in the prevention of discrete microphase separation in the whole matrix.

Mechanical Properties

The stress–strain behavior the TPEE samples provided clues for further understanding their morphology. Figure 9 shows the stress–strain curves of TPEEs with different SS/HS ratios from 50:50 to 30:70. The stress–strain characteristics of the TPEEs prepared with only BDO were typical of thermoplastic elastomers, especially when the SS/HS ratios were 50:50 and 40:60. Their shapes greatly changed with the SS/HS ratio and with composition of CE; at low concentrations of the minor CE, the sample showed the typical stress–strain curves of elastomers with higher toughness imparted to the material, whereas a further increase in the minor CE deteriorated both the tensile and strain properties and finally led to losses in their elastomeric properties. Most of the samples showing elastomeric characteristics showed a small (several percentage) and linear elastic domain followed by a well-defined yield point, typical of thermoplastic behavior. The tensile strength at break of 5/5PH-10 was about 50 MPa; this was the highest mechanical strength among all of the TPEE samples. Moreover, 5/5PH-10 showed the highest ultimate elongation (1100–1300%) among these samples.

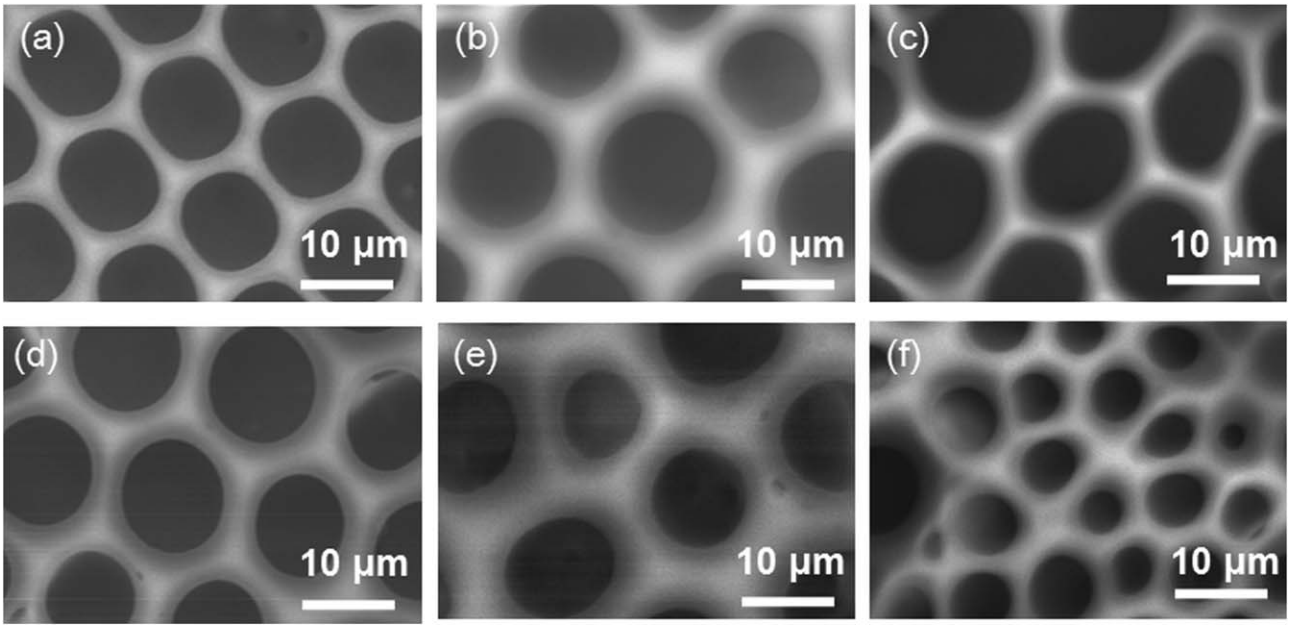

Figure 9. SEM images of honeycomb-structured, porous films fabricated with (a) 5/5PH-10, (b) 6/4PH-10, (c) 7/3PH-10, (d) 5/5PT-10, (e) 6/4PT-10, and (f) 7/3PT-10 with a polymer concentration of 0.1 g/dL in $CHCl_3$. The scale bar represents 10 μm.

The stress–strain response exhibited by the TPEE samples was dependent on their relative segment compositions. According to DMTA of 5/5PB, 5/5PH-10, and 5/5PT-10, their morphologies were comprised of microphase-separated polyester domains dispersed in an amorphous matrix, compositionally dominated by PTMEG segments. In these samples, the long-range connectivity of the hard domains was limited because of their relatively low HS contents. Accordingly, the dispersed crystalline HS domains preferentially served as physically crosslinked regions for the amorphous SS matrix and enabled 5/5PB, 5/5PH-10, and 5/5PT-10 to behave as elastomers. They exhibited low Young's moduli and remarkably high elongations at break. The increase in the amount of minor CE may have reduced the distinct crystalline region and resulted in the deterioration of the mechanical properties. The 7/3PB and 7/3PT-10 samples showed a sharp yield point with higher Young's moduli than the other samples with lower HS ratios, and their elongations at break were remarkably lower than those of the other members of the series. Such behavior suggested an increase in the hard-phase connectivity/percolation of the TPEEs with increasing polyester amount. In

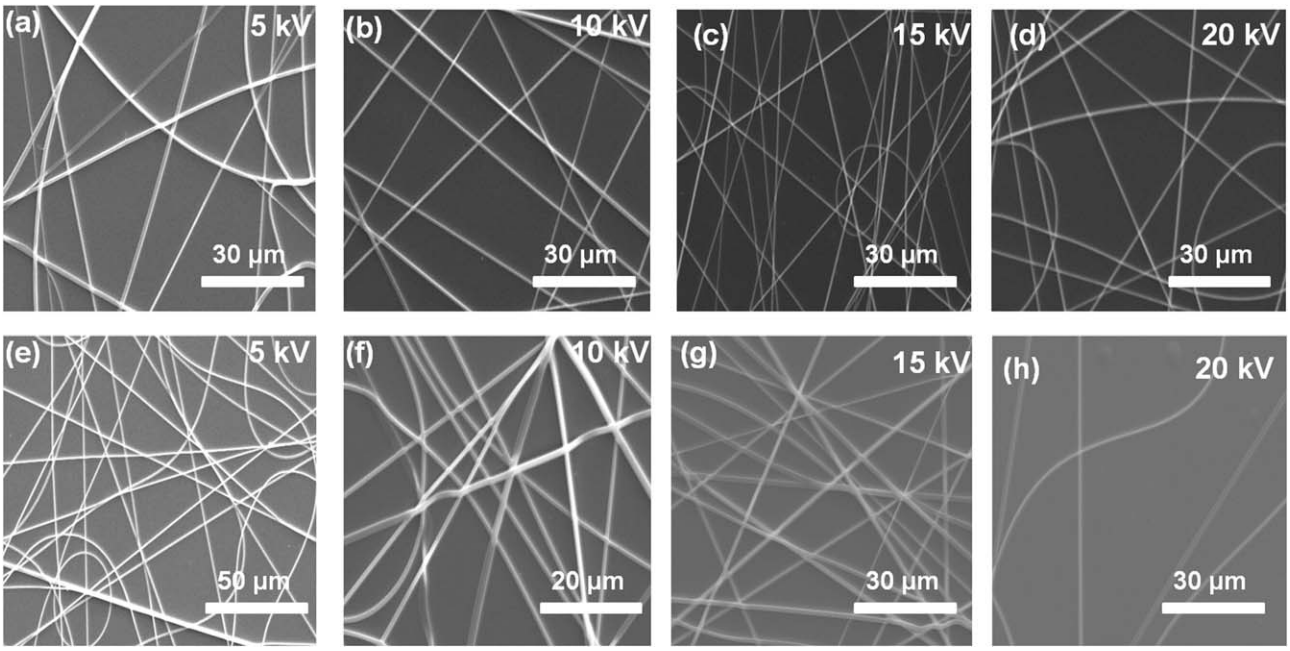

Figure 10. SEM images of the electrospun fibers of (a–d) 5/5PT-10 and (e–h) 5/5PH-10 samples with various voltages from 5 to 20 kV.

addition, as the amount of minor CE increased, the randomness of the HS domains increased as well. Thus, all of the samples with SS/HS ratios of 30:70, except for 7/3PT-10, seemed to act more like hard thermoplastics rather than elastomers.

Fabrication of the Honeycomb Pattern and Electrospun Fibers

The TPEEs of this study were segmented poly(ether ester) block copolymers with segments of PTMEG joined by ester bonds from NDC polyester segments. The use of different types of minor CE made the HS domain complicated and, thus, led to changes in the molecular mobilities of the HSs and, particularly, their immiscibility. This caused phase separation and the formation of an amorphous soft phase of polyether-rich segments and hard crystalline polyester domains with high T_m values. It may be challenging with such materials with highly compositional heterogeneities to fabricate uniform structures on the nanometer or micrometer scale. For example, honeycomb-structured porous films were prepared with breath figures.[30]

Because water droplets acted as templates for pores in this process, the water droplet size and, therefore, the size of the pores were influenced by the casting conditions and the polymer used.[27,30] Recently, a range of honeycomb-structured, porous films were successfully manufactured with a range of polymers, including block copolymers and amphiphilic random copolymers. However, it was hard to find previous studies applying condensation polymers to the fabrication of uniform porous films. The polymer properties, such as the average MW, degree of branching, end groups, and impurities such as unreacted monomer, solvents, and low-MW fractions, affected the chain flexibility and influenced the pore size, precipitation, and stabilization of the water droplets. Figure 10 shows the SEM images of the honeycomb-structured porous films fabricated by the 5/5PH-10, 5/5PT-10, 6/4PH-10, 6/4PT-10, 7/3PH-10, and 7/3PT-10 samples. By tuning various conditions such as the relative humidity, polymer concentration, and drying rate, we clearly observed porous films with various uniformities on the basis of the composition and microstructure of the polymers. The 5/5PH-10, 5/5PT-10, and 6/4PH-10 samples gave hexagonally close packed pores with average pore size diameters of about 5 μm; however, the 6/4PT-10, 7/3PH-10, and 7/3PT-10 samples yielded porous films with nonuniform shapes and sizes. The samples with a high ratio of HSs in this study had relatively poorer hydrophilicities and microphase segregation characteristics. Because the regularity of the pores was dependent on the hydrophobic to hydrophilic ratio because of the strong interaction between water and the hydrophilic part of the polymers, the formation of uniform porous films seemed to correlate with the degree of hydrophilicity of the backbone of the TPEE elastomers and its biphasic nature driving self-assembly.

Lots of different types of polymers have been successfully electrospun into fibers, electrospun polymer fibers with diameters as small as 5 nm have also been reported, and their promising features have been demonstrated in both medical and industrial applications.[31] The polymer solution viscosity is an important parameter, which influences the spinnability. Because different polymers have different spinnable viscosity ranges, the solution viscosity may not be a controlling parameter. Moreover, evidence exists that not every polymer solution can be electrospun into nanofibers. No report has been published on electrospun TPEE nanofibers. With various important parameters taken into consideration, the preoptimal conditions were sought to yield continuous TPEE fibers. For the fabrication of TPEE fibers, the samples were dissolved in a trifluoroacetic acid/dichloromethane (TFA/DCM) (8 : 2) solvent at a concentration of 30% w/v at room temperature. Figure 10 shows SEM images of the electrospun fibers of 5/5PH-10 and 5/5PT-10 at various voltage impacts (5–20 kV). The diameter of the electrospun fibers fabricated by 5/5PH-10 ranged from about 0.59 to 1.3 μm, depending on the potential (which increased from 5 to 20 kV). Similarly, the diameters of those from 6/4PH-10 ranged from 0.48 to 1.25 μm with respect to voltage. In general, the diameter of the fibers increased with increasing voltage (from 5 to 20 kV), and the fibers became more uniform at higher electrical potentials. These results demonstrate that MW, MW distribution, and microstructure of the TPEEs were suitable for the successful fabrication of highly uniform electrospun fibers through the application of a conventional electrospinning technique. Because of the expected peculiar elastomeric properties of the resulting TPEE fibers, further studies to search for applications for them in technical and biomedical uses are a good topic for ongoing publication elsewhere.

CONCLUSIONS

The incorporation of a small amount of TCDO or HBHEE as a minor CE into conventional TPEE synthesized by the polycondensation of NDC with PTMEG in the presence of BDO CE greatly changed the microstructure of the polymers, especially for the grade with a high HS composition, because the additional minor CE changed the structure of the HS unit. Thus, the composition of CE influenced the T_{g2} and T_m values of the resulting TPEEs. On the basis of the DSC, WAXS, and DMTA results, it was revealed that the TPEEs contained a polyether-rich phase, a polyether ester blended phase, and a polyester-rich phase. As the amount of minor CE increased, the crystallinity of the polyester-rich HS sharply decreased; this resulted in the failure of microphase segregation and the loss of elastomeric properties. Accordingly, the tensile strength and elongation were able to be optimized simply through the modulation of the type and amount of minor CE. The HBHEE-incorporated 5/5PH-10 elastomer showed higher T_m values, elongations, tensile strengths, and crystallinities than the TCDO-incorporated counterpart 5/5PT-10 and values even better than those of 5/5PB, synthesized with only BDO. The application of a breath figures technique to the 5/5PH-10 and 5/5PT-10 samples yielded highly uniform honeycomb-structured porous films pores about 5 μm in diameter. In addition, electrospun fibers with diameters ranging from 0.3 to 1.3 μm were successfully fabricated with the same elastomers.

ACKNOWLEDGMENTS

This work was supported by the Fundamental R&D Program (contract grant number 10037176) for Core Technology of Materials, which is funded by the Ministry of Knowledge Economy of the Republic of Korea.

REFERENCES

1. Legge, N. R.; Holden, G.; Schroeder, H. Thermoplastic Elastomers: A Comprehensive Review; Carl Hanser: Munich, **1987**; Chapters 8 and 9.
2. Weidisch, R.; Gido, S. P.; Uhrig, D.; Iatrou, H.; Mays, J.; Hadjichristidis, N. *Macromolecules* **2001**, *34*, 6333.
3. Gabrielse, W.; Soliman, M.; Dijkstra, K. *Macromolecules* **2001**, *34*, 1685.
4. Stribeck, N.; Sapoundjieva, D.; Denchev, Z.; Apostolov, A. A.; Zachmann, H. G.; Stamm, M.; Fakirov, S. *Macromolecules* **1997**, *30*, 1329.
5. Amin, S.; Amin, M. *Rev. Adv. Mater. Sci.* **2011**, *29*, 15.
6. Szymczyka, A.; Nastalczyka, J.; Sablongb, R. J.; Roslaniec, Z. *Polym. Adv. Technol.* **2011**, *22*, 72.
7. Fakirov, S. In Handbook of Condensation Thermoplastic Elastomers; Fakirov, S., Ed.; Wiley-VCH: Weinheim, **2005**; Chapter 6, p 167.
8. Wolfe, J. In Multiphase Polymers; Advances in Chemistry Series 176; Cooper, S., Estes, G., Eds.; American Chemical Society: Washington, DC, **1979**; p 129.
9. Park, Y. H.; Kim, K. Y.; Han, M. H. *J. Appl. Polym. Sci.* **2003**, *88*, 139.
10. Roslaniec, Z.; Slonecki, J.; Wojcikiewicz, H. Pol. Pat. 158339 (**1991**).
11. Matsuki, T.; Kuwata, J.; Takayama, H. Jpn. Pat. 01095127 (**1989**).
12. Tamura, S.; Matsuki, T.; Kuwata, J.; Ishii, H. Jpn. Pat. 02269118 (**1990**).
13. Pozdzal, R.; Roslaniec, Z. *Kautsch. Gummi Kunstst.* **1999**, *52*, 656.
14. Ukielski, R.; Wojcikiewicz, H. *Polimery* **1988**, *33*, 9.
15. Magryta, J.; Pyskl, L.; Roslaniec, Z.; Kapko, E. *Polimery* **1988**, *33*, 464.
16. Cai, F.; Isayev, A. I. *J. Elast. Plast.* **1993**, *25*, 74.
17. Cai, F.; Isayev, A. I. *J. Elast. Plast.* **1993**, *25*, 249.
18. Roslaniec, Z.; Poslednik, S. *Sci. Pap. Tech. Univ. Szczecin* **1988**, *14*, 217.
19. Gogeva, T.; Fakirov, S. *Makromol. Chem.* **1990**, *191*, 2355.
20. Nelsen, S. B.; Gromelski, S. J.; Charles, J. J. *J. Elast. Plast.* **1983**, *15*, 256.
21. DS BIOVIA. Materials Studio overview. http://accelrys.com/products/materials-studio/index.html (accessed May 28, 2015).
22. Pierre, E.; Laurent, R.; Laurent, B.; Maud, S. *Eur. Polym. J.* **2012**, *48*, 1001.
23. Geissler, M.; Xia, Y. N. *Adv. Mater.* **2004**, *16*, 1249.
24. Sokuler, M.; Auernhammer, G. K.; Roth, M.; Liu, C. J.; Bonaccurso, E.; Butt, H. F. *Langmuir* **2010**, *26*, 1544.
25. Dersch, R.; Steinhart, M.; Boudriot, U.; Greiner, A.; Wendorff, J. H. *Polym. Adv. Technol.* **2005**, *16*, 276.
26. Ilona, K.; Claudia, H.; Reiner, M. K.; Rolf-Joachim, M.; Wolf-Dieter, D. *Appl. Environ. Microbiol.* **1998**, *64*, 1731.
27. John, J. V.; Moon, B. K.; Kim, I. *React. Funct. Polym.* **2013**, *73*, 1213.
28. Chuah, H. H.; Lin-Vien, D.; Soni, U. *Polymer* **2001**, *42*, 7137.
29. Szymczyk, A. *Eur. Polym. J.* **2009**, *45*, 2653.
30. Escale, P.; Ting, S. R. S.; Khoukh, A.; Rubatat, L.; Save, M.; Stenzel, M. H.; Billon, L. *Macromolecules* **2011**, *44*, 5911.
31. Huang, Z.-M.; Zhang, Y.-Z.; Kotakic, M.; Ramakrishna, S. *Compos. Sci. Technol.* **2003**, *63*, 2223.